Academic Journal of Science and Technology
ISSN: 2771-3032 | Vol. 20, No. 3, 2026

Lightweight Design and Manufacturing of High-Pressure Die-Cast Magnesium Alloy Components for Automotive Applications: A Comprehensive Review

Xingchu Xiang[1], Junchi Ma[2], Rui Hua[1]

[1]Anhui Jianghuai Automobile Group Co., Ltd, Hefei 230000, China
[2]School of Mechanical Engineering, Hefei University of Technology, Anhui 230009, China

Abstract: The imperative for vehicle mass reduction, driven by increasingly stringent greenhouse gas emission regulations and the rapid proliferation of electric vehicles, has positioned magnesium (Mg) alloys as compelling candidates for structural automotive applications. With a density of merely 1.74 g/cm^3 — approximately two-thirds that of aluminium and one-quarter that of steel — Mg alloys offer an unparalleled weight advantage among engineering metals. High-pressure die casting (HPDC) remains the dominant manufacturing route for automotive Mg components, accounting for approximately 90% of total production volume. This review systematically synthesizes findings from peer-reviewed publications to establish a comprehensive knowledge framework encompassing alloy systems, vehicular applications, and original equipment manufacturer (OEM) development practices. In the domain of alloy selection, the Mg-Al-Zn system (principally AZ91) provides superior castability and strength for non-safety-critical components, whereas the Mg-Al-Mn system (AM50/AM60) delivers the requisite balance of strength and ductility for crash-relevant structures such as seat frames and instrument panel beams. Recent advances in Mg-Al-Sn (AT72) and Mg-Al-Zn-Mn alloy families demonstrate promising avenues for tailored strength–ductility combinations. With respect to vehicular deployment, Mg die castings have been successfully implemented across body systems (door inners, front-end carriers, closure panels), achieving mass reductions of 40–50%, and chassis systems (wheels, steering columns, subframes). A detailed case study of the Mg alloy seat frame (MASF) forward-development programme at Changan Automobile illustrates the complete design–simulation–process–verification chain, yielding a 9.88 kg seat frame representing a 24.6% mass reduction with process yields exceeding 90%. The challenges and future prospects for expanded automotive Mg adoption are critically assessed.

Keywords: Magnesium alloys; high-pressure die casting; automotive light-weighting; structural applications.

1. Introduction

Magnesium (Mg) is the lightest structural metal available for engineering applications, possessing a density of 1.74 g/cm^3, which is approximately 33% lower than aluminium alloys and 75% lower than steel [1–3]. The specific strength and specific stiffness of Mg alloys are comparable to or exceed those of aluminium, and substantially surpass engineering plastics [4,5]. Coupled with superior vibration damping characteristics — at 100 MPa stress, the attenuation coefficient of AM60 reaches 72%, compared with merely 4% for aluminium alloy A380 [6] — and excellent electromagnetic shielding properties, Mg alloys present a uniquely attractive materials proposition for vehicular lightweighting.

The contemporary automotive industry operates under progressively stringent emissions constraints. The corporate average fuel economy (CAFE) regulations in North America, the European Union's CO^2 fleet targets, and China's dual-carbon strategy collectively mandate substantial reductions in vehicle energy consumption [7,8]. In this context, lightweighting has emerged as one of the most effective technological pathways for improving fuel efficiency in internal combustion engine vehicles and extending driving range in battery electric vehicles (BEVs). Industry projections indicate that average North American vehicle Mg content, approximately 5 kg as of 2015, is expected to triple by 2025 [9].

Among the various forming processes available for Mg components, high-pressure die casting (HPDC) is the dominant manufacturing route, accounting for approximately 90% of Mg alloy products in automotive applications [10,11]. HPDC capitalises on the exceptional fluidity and minimal die affinity of Mg alloys — the latter arising from the negligible solubility of iron in magnesium — to produce large, thin-walled, geometrically complex castings with near-net-shape precision and high dimensional repeatability [12,13]. Since the landmark introduction of the first high-volume one-piece die-cast Mg alloy cross car beam (CCB) by General Motors in 1996, which achieved a 32% mass saving over the incumbent steel design [14], Mg HPDC components have been deployed across instrument panel structures, seat frames, steering armatures, door inners, front-end carriers, and liftgate assemblies [15–18].

Nevertheless, the widespread adoption of Mg alloys in the automotive sector continues to face several significant challenges: elevated raw material costs relative to steel and aluminium; limited corrosion resistance, particularly galvanic corrosion susceptibility in multi-material joints; a narrow range of commercially available alloy grades; an underdeveloped supplier ecosystem; and insufficient OEM confidence in Mg product development methodologies [6,19]. Recently, the advent of giga-casting technology, pioneered by Tesla and subsequently adopted by manufacturers including XPENG, ZEEKR, Xiaomi, and AITO with ultra-large HPDC machines exceeding 100,000 kN locking force, has created new opportunities for thin-walled, large-format Mg castings [20]. Concurrently, the development of novel alloy systems

— including high-ductility Mg-Al-Zn-Mn compositions and high-thermal-conductivity Mg-Al-RE alloys — is expanding the material design space [21,22].

2. Magnesium Alloy Material Systems

Material selection for thin-walled, large-format Mg HPDC components must reconcile three competing requirements: castability, mechanical performance, and cost [20]. The commercially available HPDC Mg alloys are predominantly based on the Mg-Al system and can be classified into three principal families: Mg-Al-Zn (typified by AZ91), Mg-Al-Mn (typified by AM50/AM60), and Mg-RE (typified by WE43/WE54) [23–27]. For automotive cockpit components, which operate in semi-enclosed environments without stringent corrosion demands, material selection primarily targets the optimisation of mechanical properties and casting process compatibility. The following subsections examine the two alloy families most extensively employed in automotive HPDC applications.

2.1. Mg-Al-Zn Alloys

The Mg-Al-Zn alloy series, encompassing AZ91, AZ31, and AZ61, constitutes the most extensively studied and historically established Mg alloy family [28]. AZ91, containing approximately 9 wt% aluminium, is the most widely used HPDC Mg alloy by virtue of its favourable castability, good tensile properties, and the lowest raw material cost among commercial Mg alloys [6,29]. It has served as the material of choice for transmission housings, central control brackets, cylinder head covers, and steering column brackets for several decades [30]. Figure 1 presents a comparative assessment of weight and rigidity metrics across different wheel materials and manufacturing technologies, demonstrating the inherent advantage of Mg alloys in the weight domain.

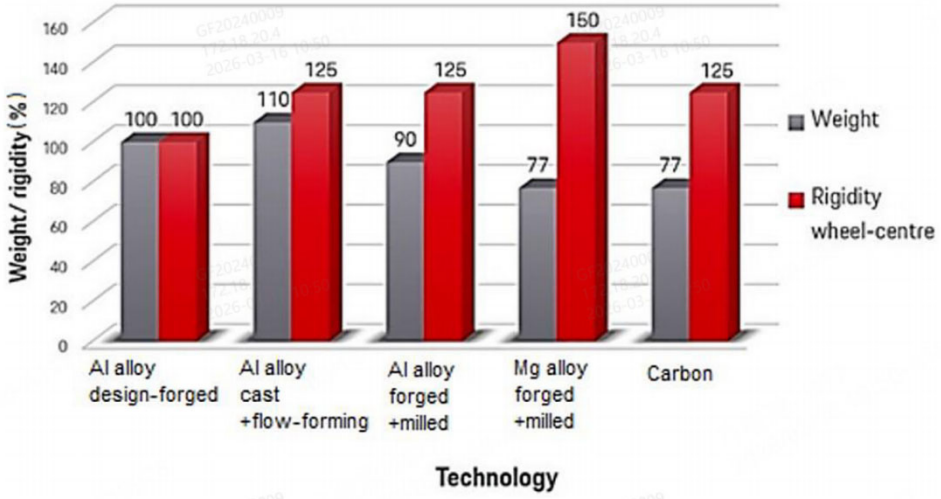

Figure 1. Weight and rigidity comparison of different wheel materials and manufacturing technologies. Mg alloy forged + milled wheels exhibit the lowest weight index among all configurations evaluated.

Table 1 summarises the mechanical properties of AZ91 alloy under various processing conditions and with microalloying additions. In the as-cast HPDC condition, AZ91 exhibits a yield strength (YS) of 95–160 MPa, an ultimate tensile strength (UTS) of 135–250 MPa, but a limited elongation (EL) of only 2–7%, which constitutes its principal shortcoming [20,31]. Heat treatment (T4 or T6) improves strength but yields only marginal elongation gains. Notably, the addition of 0.5 wt% yttrium to AZ91 achieves a UTS of 270 MPa with an elongation of 10%, representing a markedly improved strength–ductility synergy [32].

Table 1. Summary of mechanical properties of AZ91-series alloys under various conditions.

Alloy	Condition	YS (MPa)	UTS (MPa)	EL (%)
AZ91	As-cast	95	135	2
AZ91	T4	80	230	4
AZ91	T6	120	200	3
AZ91	T6	130	154	1.9
AZ91+1.0Ce	HPDC	158	248	6.8
AZ91+0.5Y	HPDC	162	270	10
AZ91+1.0Nd	HPDC	164	258	5.6
AZ91	Pre-heated + WQ	125	282	22

From a process perspective, AZ91 offers excellent casting fluidity suitable for geometrically complex components.

However, its relatively low as-cast ductility renders it inadequate for crash-relevant structural members requiring significant energy absorption capacity, such as seat frames and door inners. Consequently, AZ91 is preferentially deployed in components with benign operating conditions, including centre console brackets and DVD support frames [20]. Multi-attribute decision-making (MADM) analysis has confirmed AZ91 as the most suitable alloy for wheel applications across a range of candidate Mg compositions [35].

Recent alloy development efforts have yielded promising new HPDC compositions. The Mg-Al-Sn system, exemplified by AT72 (Mg-7Al-2Sn), achieves a UTS comparable to AZ91 with an elongation of 8.3% — approaching that of AM60B — through strengthening by Mg^2Sn precipitates [21]. Furthermore, a newly developed Mg-Al-Zn-Mn alloy family (Figure 2), with 4–5% Al and 0.4–1.2% Zn, enables tailored strength–ductility combinations through compositional tuning, exhibiting superior bending ductility compared with AM60B [22].

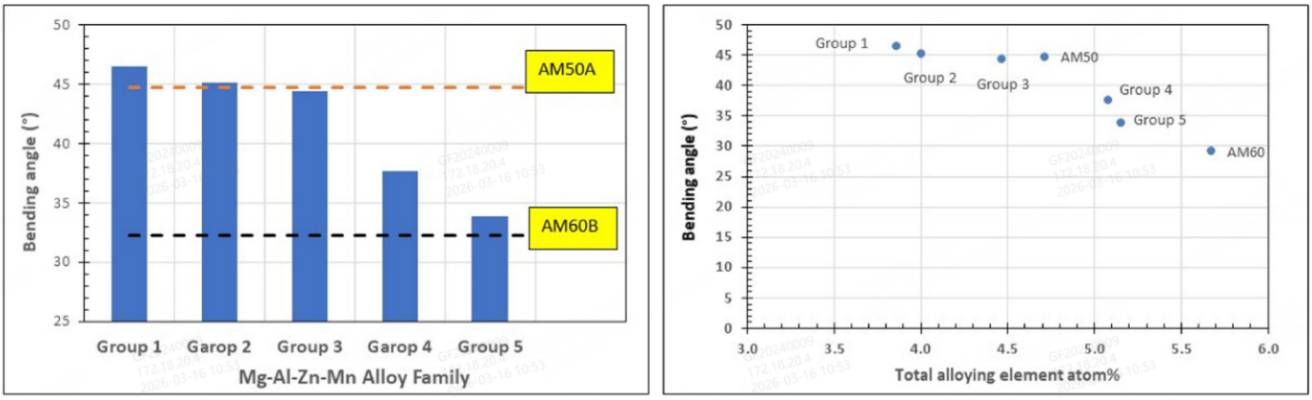

Figure 2. Bending angle comparison between the Mg-Al-Zn-Mn alloy family and conventional AM alloys. (a) Bending angle versus alloy composition. (b) Bending angle versus total alloying element content (atom%), showing a threshold at ~5 atom%.

2.2. Mg-Al-Mn Alloys

The Mg-Al-Mn series alloys represent the second principal alloy family employed in automotive cockpit structural components. AM50 and AM60 have attracted considerable attention owing to their relatively superior combination of strength and elongation compared with AZ91. The enhanced corrosion resistance and toughness of AM-series alloys are attributable to the reduction of aluminium content and the addition of manganese, which, while improving ductility and corrosion performance, entails a trade-off in castability and absolute strength [36–38]. At present, AM50 and AM60 constitute the predominant materials for automotive seat frames and cross car beams [20].

Table 2. Summary of mechanical properties of AM50/AM60-series alloys.

Alloy	Condition	YS (MPa)	UTS (MPa)	EL (%)
AM50	HPDC	125	210	10
AM50	As-extruded	168	268	18
AM50+0.15B	As-cast	94	215	12.3
AM50+1Ce	HPDC	98	168	4.8
AM60	HPDC	115	205	6
AM60+0.2Ti	As-cast	—	284	11.2
AM60+0.9Nd	As-cast	127	230	14.0
AM60B	HPDC	130	220	8

As Table 2 demonstrates, the yield strength of AM50/AM60 is generally lower than that of AZ91, whereas their elongation is appreciably superior. Typical AM60B HPDC components achieve 6–8% elongation, conferring a significant advantage in crash energy management. AM60B has been successfully deployed in seat frames (e.g. Changan E01, Alfa Romeo 156) and cross car beams (e.g. Ford Explorer, Voyah FREE) [6,18]. However, AM-series alloys are generally unsuitable for service above 150 °C, beyond which a measurable degradation in strength is observed [43].

Extensive modification studies have explored the addition of Ti, Sn, Y, Nd, Ce, and other elements to improve AM-series performance. Among these, Ti, Nd, Sn, and Ce have proven most effective for AM60 [32,44]. A particularly noteworthy finding concerns the age-hardening response of AE44 alloy with 0.3% Mn addition, wherein nanoscale Al-Mn particle precipitation achieves substantial strength enhancement under T5 conditions without appreciable loss of ductility [45]. This observation suggests that similar precipitation strengthening mechanisms may be operative in other Mn-containing Mg-Al alloys, including AM50A and AM60B.

In summary, AM-series alloys (AM50 and AM60) remain the preferred materials for die-cast automotive cockpit structural components at present. AZ-series alloys are better

suited to non-safety-critical components with favourable operating conditions. Mg-RE alloys, despite possessing excellent elevated-temperature mechanical properties, face cost barriers that preclude widespread automotive adoption [20,46]. The development of Mg alloys combining high strength, high ductility, and low cost — particularly low-cost Mg-RE compositions — represents a critical frontier for expanding automotive Mg applications.

3. Vehicular Applications of Magnesium Alloys

Mg alloy applications in the automotive domain span four principal vehicle systems: body, chassis, powertrain, and interior/exterior trim. The exceptional casting fluidity of Mg alloys confers a natural advantage for thin-walled structural components and large internal structures [6]. This section systematically catalogues current applications and development trajectories across body and chassis systems.

3.1. Body System

3.1.1. Door assemblies

Door inner panels represent among the most technically demanding thin-walled, large-format Mg die castings in the body system. Typically 2–5 mm in wall thickness [47], door inners must simultaneously resist aerodynamic wind loads, door-slam forces, hold-open forces, and general use/abuse loads, imposing stringent requirements on both structural strength and stiffness [14]. Research on Mg alloy door inners has accelerated since the 1990s, culminating in several notable production implementations. Figure 3 presents a panorama of production and concept Mg door applications across multiple OEMs.

Figure 3. Development and application of Mg alloys in car doors: (a) Aston Martin Vanquish S with cast Mg side door inner; (b) All-new 2018 Jeep Wrangler produced with a die-cast Mg rear swing gate; (c) Chrysler Pacifica showing the liftgate assembly highlighted by a Mg die-cast inner; (d) The rear end of the Mercedes-Benz E-Class T-Model featuring the hybrid Mg-Al hatch back; (e) Inner door frame of the Daimler-Chrysler SL Roadster; (f) Ford's concept die-cast Mg door inner with an open architecture; (g) Integrated Mg die-cast door inner designed as part of a DOE sponsored project led by GMC; (h) Ultra-thin and ultra-light Mg alloy door inner.

The 2017 Chrysler Pacifica liftgate inner constitutes a landmark achievement: a single one-piece Mg die casting replaced nine components from the previous generation, achieving a liftgate assembly mass reduction of nearly 50% [14,47]. Figure 4 provides further detail on the Pacifica liftgate assembly alongside the Aston Martin DB9 side door inner (estimated 43% mass reduction) and the GM-led DOE integrated door project (approximately 50% mass reduction with speaker integration).

Figure 4. Production examples of Mg die-cast closure inners: (upper left) 2017 Chrysler Pacifica with Mg liftgate assembly; (upper right) Aston Martin DB9 Mg side door inner; (lower) GM DOE-sponsored integrated Mg door inner versus equivalent steel stamped door.

From a design standpoint, Mg closure inners exploit the alloy's molten-state fluidity and capacity for deep-rib

geometries to achieve one-piece designs incorporating local ribbing, integrated gussets, and variable-thickness sections tailored to stiffness and crash targets [14]. Galvanic corrosion between Mg and dissimilar metals is mitigated through multi-material strategies: typically, an aluminium sheet outer panel is bonded to the Mg inner via adhesive and hemming, while the Mg casting receives an offline conversion coating and powder coat prior to assembly [14,47].

3.1.2. Front-end carriers and front upper components

Substitution of hydraulically formed steel, tubular steel, or extruded aluminium with die-cast Mg for front-end carriers yields substantial mass reduction at the vehicle's front axle, with direct benefits for handling dynamics and axle-load distribution [6]. Figure 5 compiles representative front-end carrier and front upper component applications spanning Tesla, Porsche, Land Rover, Jaguar, Mercedes-Benz, and Audi.

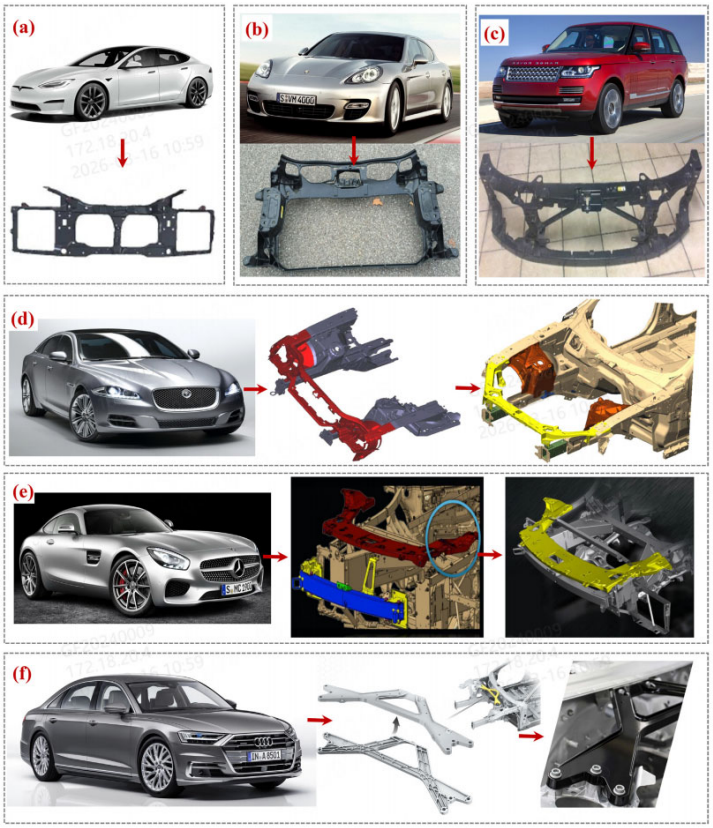

Figure 5. Mg alloy front-end carrier and front upper component applications: (a) Tesla Model S one-piece die-cast Mg front-end carrier (6.49 kg); (b) Porsche Panamera G2 front-end carrier (AM50A, 3.5 kg saving); (c) Range Rover front-end carrier (AM60B, 7.1 kg saving); (d) Jaguar XJ front upper component (AM60B, 30% mass reduction); (e) Mercedes-Benz AMG GT front upper component (AM60B, 3.5 kg); (f) Audi A8 cabin bracket (28% mass reduction).

Table 3. Representative Mg alloy front-end carrier and front upper component applications.

Vehicle	Year	Mass (kg)	Material / Key Features
Tesla Model S	2012	6.49	One-piece die-cast Mg front-end carrier
Porsche Panamera G2	2010	3.50	AM50A; 3.5 kg mass saving
Range Rover	2012	7.10	AM60B; significant mass reduction
Jaguar XJ	2009	4.90	AM60B front upper; 30% mass reduction vs. Al-tube
Mercedes AMG GT	2015	3.50	AM60B front upper; bolted assembly
Changan ENDO EV460	2020	3.19	AM60B front-end carrier

3.1.3. Engine hoods and trunk lids

Exploratory applications of Mg alloys in engine hoods and trunk lids date to the 1950s, when General Motors fabricated a prototype hood for the Buick LeSabre (1951) and various body panels for the Chevrolet Corvette SS (1957) [6]. More recently, Volkswagen developed Mg alloy prototype trunk lids and hoods for the Lupo, achieving 50% mass reduction versus steel and 15–20% versus aluminium, with reinforcements (hinges, locks) joined by punch-riveting and inner/outer panels bonded by heated adhesive [48,49]. Figure 6 illustrates several representative closure and roof applications.

Figure 6. Mg alloy applications in roof panels, engine hoods, and trunk lids: (a) Mercedes-Benz SL/SLK series folding Mg roof; (b) Chrysler Mg-intensive body inner panel; (c) Mercedes E-Class touring trunk lid (AM50); (d) VW Lupo Mg trunk lid and hood prototypes.

3.2. Chassis System

3.2.1. Wheels

Mg alloy wheels represent one of the earliest and most established automotive applications of Mg alloys [50]. Offering 30–40% mass reduction compared with aluminium and 60–75% versus steel, Mg wheels — as unsprung, rotating components — exert a direct and disproportionate influence on vehicle handling, ride comfort, and braking performance [51]. Cast Mg wheels commonly employ AZ91, AM50/AM60, AE44, and ZK61, while wrought (forged) wheels utilise AZ31, AZ61, AZ80, and ZK30/ZK60 [50]. Figure 7 presents a comprehensive overview of Mg wheel applications and manufacturing processes.

Figure 7. Mg alloy wheel applications and manufacturing processes: (a) Chevrolet Corvette low-pressure cast wheel; (b) Cadillac CT4-V forged-spun wheel; (c) AMG Project One bionic-design forged wheel; (d–f) AZ80 hollow-billet extruded wheels; (g) Bugatti Chiron Super Sport 300+; (h) Porsche 911 GT3 RS forged wheel; (i) Bandit9 electric racing wheel; (j) Forward-and-reverse extrusion forming process.

Recent high-profile deployments include the first mass-produced forged-spun Mg wheels for the 2022 Cadillac CT4-V BLACKWING, the AMG Project One's patented bionic-design 9-spoke forged wheels, and the Porsche 911 GT3 RS forged Mg wheels (8 kg saving) [6]. On the process innovation front, Wang et al. developed a hollow-billet extrusion method and a one-step forward-and-reverse extrusion technique, providing industrially scalable routes for one-piece Mg wheel production [52,53].

3.2.2. Steering wheels

The Mg alloy steering wheel skeleton enjoys the highest global recognition and acceptance among automotive Mg components, owing to the material's exceptional energy absorption and vibration damping properties [54]. Die casting is the prevailing manufacturing method, with the elimination of welding operations conferring cost advantages that have driven adoption by numerous OEMs. Figure 8 illustrates representative Mg steering wheel applications including production skeletons and crashworthiness evaluation.

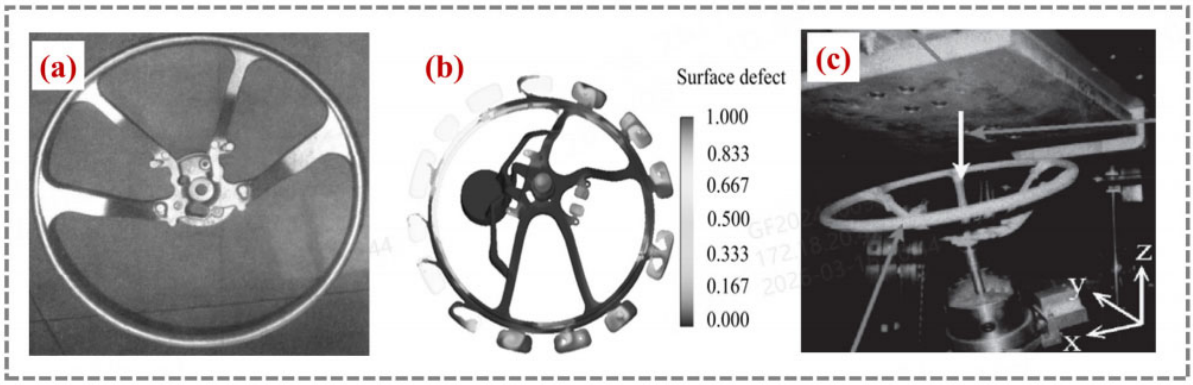

Figure 8. Mg alloy steering wheel applications: (a) Mg steering wheel skeleton produced by Chongqing Magnesium Industry for Shanghai GM; (b) Surface defect probability simulation; (c) Steering wheel crash test.

3.2.3. Subframes

Mg alloy subframes represent the most effective pathway for chassis structural lightweighting, additionally offering road-vibration isolation and improved stability [55]. Figure 9 presents three landmark applications: the 2005 Corvette Z06 Mg front crossmember (replacing Al brackets for weight and fuel savings) [56], the Audi R8 AZ91 rear subframe (HPDC), and the 2016 Ford Focus AE44 cast Mg subframe (32% mass reduction versus the equivalent steel frame, with all joints validated through bolt-load-retention and corrosion testing) [57].

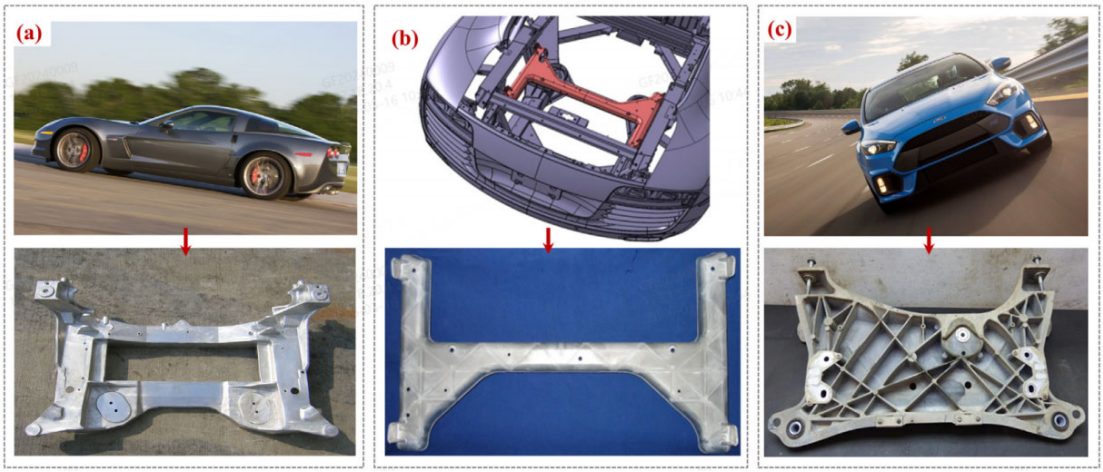

Figure 9. Mg alloy subframe applications: (a) Corvette Z06 Mg front crossmember; (b) Audi R8 AZ91 rear subframe; (c) 2016 Ford Focus AE44 Mg subframe (32% mass reduction).

4. OEM Development Case Study

To provide actionable insight into Mg alloy component development practice and enhance industry confidence in mass-production feasibility, this section presents a detailed case study of the Mg alloy seat frame (MASF) programme at Changan Automobile, documented by Yang et al. [11] and Liu et al. [6]. This programme adopted a complete forward-development methodology, utilising the vehicle body environment as the design boundary to carry the MASF through design, simulation, manufacturing, and validation.

4.1. Forward Development Framework

The MASF forward-development framework (Figure 10) encompasses four principal stages: (i) concept design and simulation — including structural design, static strength

analysis, seatbelt anchorage strength analysis, and modal analysis; (ii) mould design and development — encompassing mould-flow analysis, process optimisation, die casting machine selection, and gating system design; (iii) prototype production — covering mould opening and repair, material preparation, die casting, and flash trimming; and (iv) quality testing and performance analysis — including flaw detection, microstructural and mechanical property characterisation, seatbelt anchorage testing, and seat back and headrest testing [11].

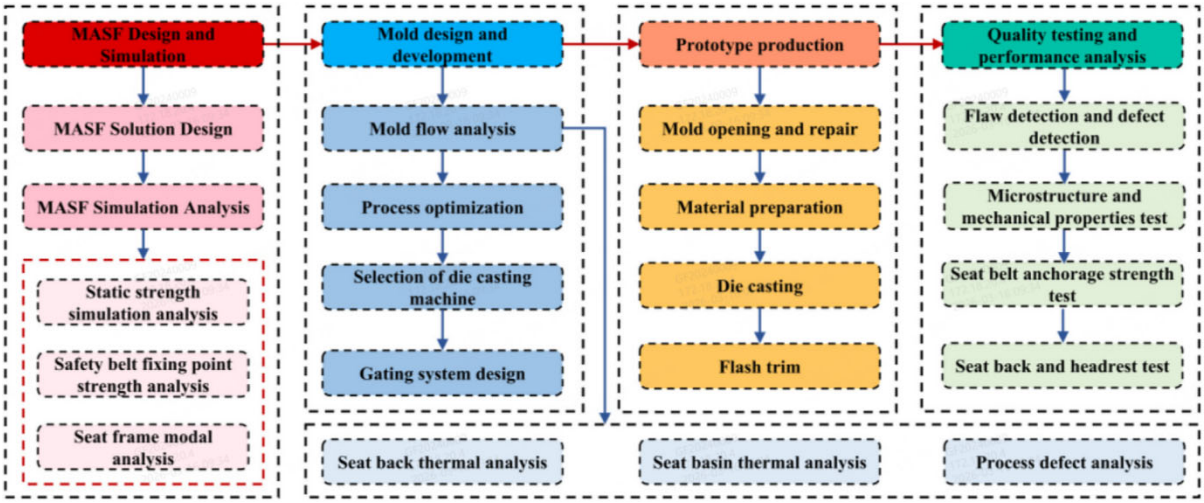

Figure 10. Complete forward-development framework for the MASF programme, spanning four stages: design and simulation, mould design and development, prototype production, and quality testing and performance analysis.

4.2. Structural Design

The MASF structural design introduces a novel headrest–backrest integrated configuration that achieves a balance between lightweight performance and occupant safety. Both the seat back and seat basin are die-cast Mg alloy structures, with side panels, floating steel wires, adjustment components, and slide rails fabricated from steel (Figure11). Compared with conventional stamped-and-welded steel seats, the MASF offers substantially higher structural integration, a reduced component count, and a simplified production process. AM60B alloy was selected as the casting material on the basis of its high tensile strength and superior energy absorption capacity [6,11].

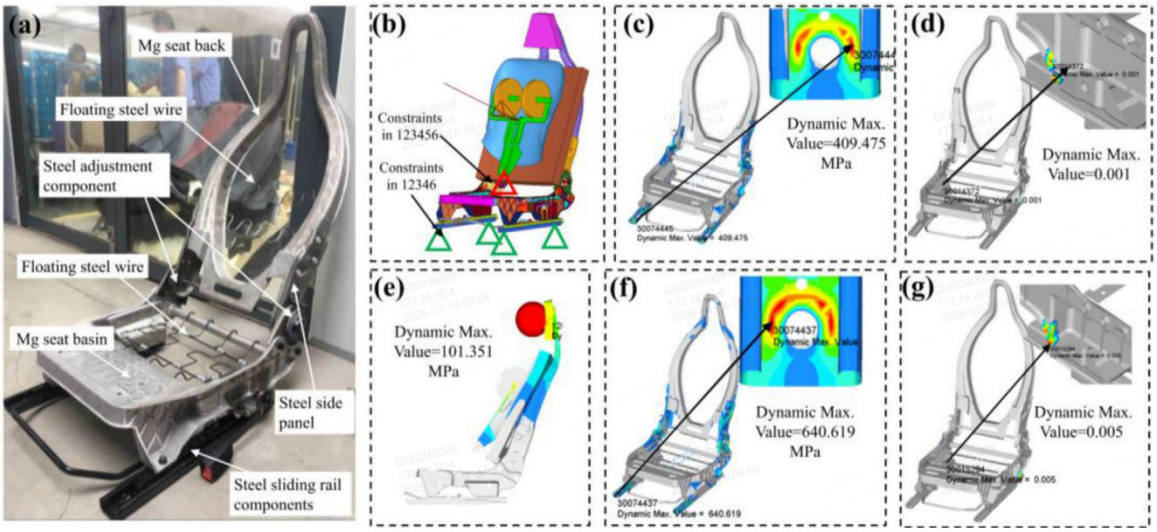

Figure 11. MASF structure and static strength simulation results: (a) MASF assembly structure showing Mg seat back, seat basin, and steel functional components; (b) Seat back boundary conditions and loading configuration; (c) Seat back stress distribution (max. 409.5 MPa); (d) Seat back strain distribution (max. 0.001); (e) Headrest loading method; (f) Headrest stress distribution (max. 640.6 MPa); (g) Headrest strain distribution (max. 0.005).

The final manufactured MASF weighs 9.88 kg, representing a mass reduction of 3.23 kg (24.6%) relative to the baseline sheet-metal seat. Under stable die casting conditions, the seat basin achieves a process yield of 96% and the seat back 92%, with scrap primarily attributable to parameter instability causing poor filling, such as slight cold-shut defects observed at the seat back gating end [11].

4.3. CAE Performance Analysis

Computational analysis constitutes the core of the MASF development process, encompassing three domains: static strength, seatbelt anchorage strength, and modal analysis [6,11]. Figure 12 presents the seatbelt fixed-point strength analysis with design optimisation (upper panel) and the three modal analysis modes (lower panel).

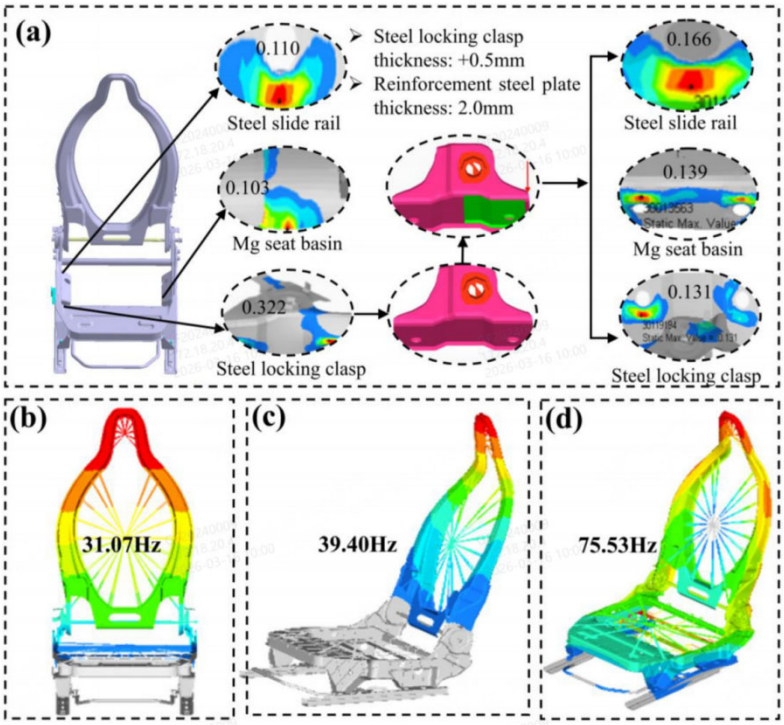

Figure 12. MASF optimisation and modal simulation results: (a) Seatbelt fixed-point strength analysis showing locking clasp strain optimisation from 0.322 to 0.131 through thickness increase and reinforcement plate addition; (b) First mode: lateral oscillation at 31.07 Hz; (c) Second mode: longitudinal pitch at 39.40 Hz; (d) Third mode: torsion at 75.53 Hz. All modal frequencies exceed the 18 Hz resonance avoidance target.

For the static strength analysis, six degrees of freedom at the four slider mounting points were constrained, and a rearward moment of 530 N·m was applied to the upper frame. The simulation yielded a maximum stress of 409.5 MPa and maximum strain of 0.001 for the seat back, both within the target limits of 784.0 MPa and 0.167, respectively (Table 4). The headrest was loaded from 373 N to 890 N using a spherical model, producing a displacement of 101.3 mm (below the 102 mm target), maximum stress of 640.6 MPa, and maximum strain of 0.005, all within design targets.

The seatbelt anchorage analysis under 20g loading initially revealed a locking clasp strain of 0.322, exceeding the 0.30 material failure threshold. This deficiency was rectified by increasing clasp thickness and installing a reinforcement plate, reducing the strain to 0.131. Modal analysis confirmed all natural frequencies (31.07 Hz lateral, 39.40 Hz pitch, 75.53 Hz torsion) substantially exceed the 18 Hz resonance avoidance criterion.

Table 4. Summary of MASF CAE simulation results.

Analysis Item	Actual	Target	Status
Seat back max. stress (MPa)	409.5	≤ 784.0	Pass
Seat back max. strain	0.001	≤ 0.167	Pass
Headrest max. stress (MPa)	640.6	≤ 784.0	Pass
Headrest max. strain	0.005	≤ 0.167	Pass
Locking clasp strain (optimised)	0.131	≤ 0.20	Pass
Lateral oscillation mode (Hz)	31.07	> 18	Pass
Pitch mode (Hz)	39.40	> 18	Pass
Torsion mode (Hz)	75.53	> 18	Pass

4.4. Die Casting Equipment Selection and Process Design

To ensure effective pressure transmission to distal regions and achieve the requisite structural performance, the intensification pressure was selected at 75–80 MPa. Calculated clamping forces of 13,479 kN (seat back) and 11,766 kN (seat basin) dictated the selection of a 1,300-tonne horizontal cold-chamber die casting machine with a 110 mm punch diameter [11].

The gating system design (Figure13) reflects the distinct

structural characteristics of each component. The seat back, a large symmetrical frame measuring 757 mm in length with V-shaped lateral depressions, employs a zonal filling strategy with internal gates positioned within the frame to promote mould compactness and thermal balance. Side gates are configured for bottom-up cavity filling to facilitate gas evacuation from deep features. The total gating system volume is 1,083.4 cm^3 (58% of shot volume), yielding a process yield of 42%. The simpler seat basin utilises a conventional four-sprue design with a system volume of 1,112.9 cm^3 (52% of shot volume) and 48% process yield.

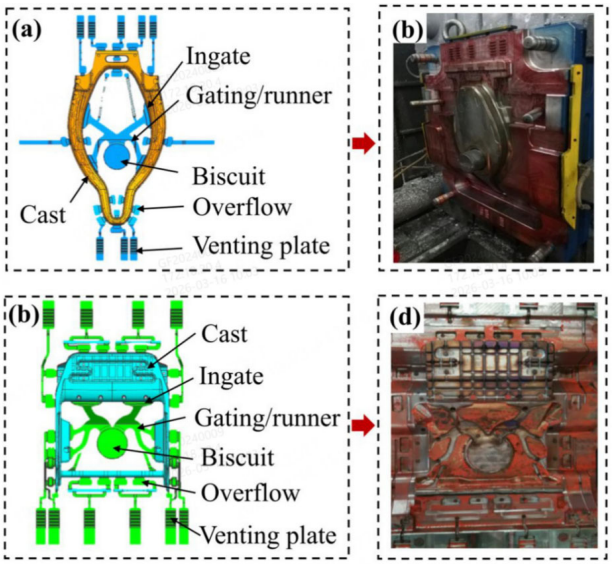

Figure 13. MASF gating system design: (a) Seat back gating scheme showing ingate, gating/runner, biscuit, overflow, and venting plate; (b) Seat back gating mould; (c) Seat basin gating scheme; (d) Seat basin gating mould.

Mould-flow simulation results (Figure 14) confirm favourable filling characteristics for both components. The seat back achieves complete cavity filling in 0.041 s with good synchronisation across all branch gates and smooth melt-flow patterns. The seat basin fills in 0.036 s with clearly defined filling regions. Process defect analysis identifies the far-gate position of the seat back as the zone of longest air residence time (exceeding 0.02 s), indicating the highest susceptibility to gas entrapment and shrinkage porosity; however, this location is non-critical from a load-bearing perspective, and targeted local cooling points at hot junctions effectively suppress porosity formation [11].

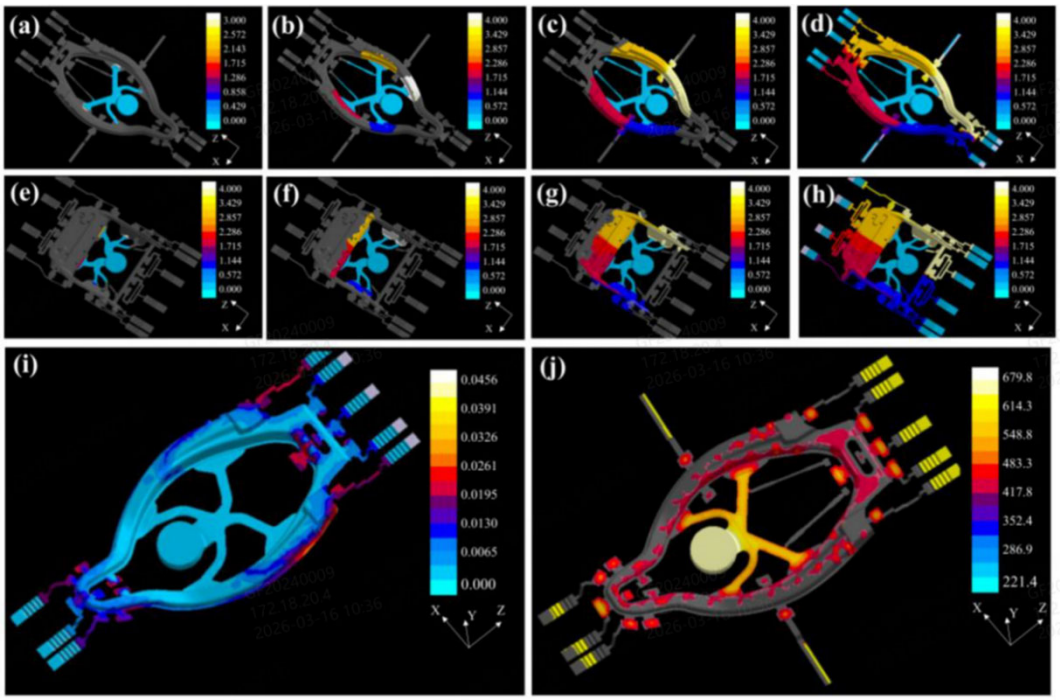

Figure 14. Mould-flow analysis results: (a–d) Material trace during seat back filling; (e–h) Material trace during seat basin filling; (i) Air contact analysis indicating gas entrapment susceptibility; (j) Temperature field analysis. Filling times: 0.041 s (seat back) and 0.036 s (seat basin).

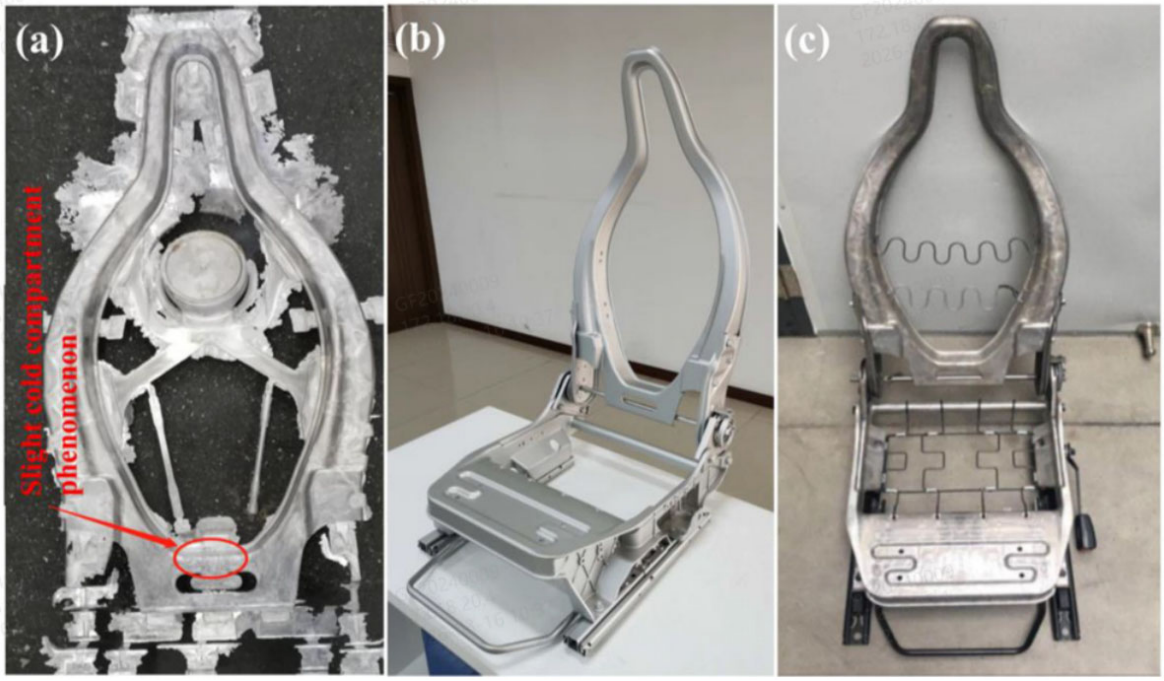

Figure 15. Final MASF products: (a) Cold-shut defect observed at gating end; (b) Completed MASF frame; (c) MASF assembly with floating steel wire. Final mass: 9.88 kg, representing a 24.6% reduction versus the baseline steel seat.

It is noteworthy that for the automotive cockpit Mg alloy components discussed herein, cold-chamber HPDC machines with locking forces of 30,000 kN are sufficient. However, since Tesla's introduction of integrated die-casting technology in 2020, ultra-large machines with locking forces exceeding 60,000–100,000 kN have been deployed by Tesla, XPENG, ZEEKR, Xiaomi, and others for oversized thin-walled aluminium vehicle body components [20]. In the future, these ultra-large die casting platforms are expected to extend to Mg alloy integrated body castings, unlocking still greater lightweighting potential.

5. Conclusions

This paper has established a comprehensive knowledge framework for automotive Mg alloy HPDC lightweight design and manufacturing, synthesised from six peer-reviewed publications spanning alloy development, vehicular applications, and OEM development practice. The principal conclusions are as follows.

(1) Alloy systems. The current automotive HPDC landscape is dominated by AZ91 and AM50/AM60. AZ91 offers superior castability and strength for non-safety-critical applications, while AM50/AM60 provides the strength–ductility balance essential for crash-relevant structures. Emerging Mg-Al-Sn (AT72) and Mg-Al-Zn-Mn alloy families demonstrate promising strength–ductility tunability. Mg-RE alloys possess excellent elevated-temperature performance but remain cost-prohibitive for high-volume automotive deployment.

(2) Vehicular applications. Mg die castings have been successfully implemented across body systems (door inners, front-end carriers, closure panels) and chassis systems (wheels, steering columns, subframes), with production examples from Tesla, Porsche, Mercedes-Benz, BMW, Jaguar, Ford, and Chrysler. One-piece die-cast door and liftgate inners achieve mass reductions of 40–50% with significant part consolidation. Front-end carriers improve axle-load distribution and handling dynamics. Forged Mg wheels have entered the options lists of premium and performance vehicles.

(3) OEM development practice. The Changan Automobile MASF programme demonstrates a complete forward-development chain from structural design through CAE simulation (static strength, seatbelt anchorage, modal analysis), die casting equipment selection, gating system design, mould-flow analysis, trial production, and qualification testing. The final product weighs 9.88 kg (24.6% mass reduction), achieves process yields exceeding 90%, and satisfies GB 14167-2013 seatbelt anchorage and GB 15083-2006/GB 11550-2009 seat and headrest test requirements.

(4) Future prospects. The principal challenges confronting expanded automotive Mg adoption include: reducing component costs; enhancing material mechanical properties, particularly through the development of low-cost, high-performance Mg-RE alloys; achieving higher degrees of part integration while controlling casting defects; and addressing in-service damage repair. The competitive pressure from ultra-high-strength steels (780–1180 MPa) and high-strength-toughness aluminium alloys demands a coordinated advance across three dimensions: material innovation (high-strength, low-cost alloy development), process innovation (giga-casting, vacuum-assisted HPDC, super-vacuum die casting), and design innovation (topology optimisation, multi-material hybrid architectures). Through such concerted efforts, the substantial lightweighting potential of Mg alloys in the automotive sector can be fully realised.

References

[1] C. Moosbrugger, L. Marquard, Engineering Properties of Magnesium Alloys, ASM International, 2017.

[2] D. Eliezer, E. Aghion, F.H. Froes, Adv. Perform. Mater. 5 (1998) 201–212.

[3] M.K. Kulekci, Int. J. Adv. Manuf. Technol. 39 (2008) 851–865.

[4] G. Ma, H. Xiao, J. Ye et al., Mater. Sci. Technol. 36 (2020) 645–653.

[5] J. Tan, S. Ramakrishna, Appl. Sci. 11 (2021) 6861.

[6] B. Liu, J. Yang, X. Zhang et al., J. Magnes. Alloys 11 (2023) 15–47.

[7] H. Friedrich, S. Schumann, J. Mater. Process. Technol. 117 (2001) 276–281.

[8] Y. Yang, X. Xiong, J. Chen et al., J. Magnes. Alloys 9 (2021) 705–747.

[9] EPA/NHTSA, Draft Technical Assessment Report, Midterm Evaluation of Light-Duty Vehicles GHG Emission Standards and CAFE Standards for MY 2022–2025, 2016.

[10] A.A. Luo, J. Magnes. Alloys 1 (2013) 2–22.

[11] J. Yang, K. Wang, Q. Yang et al., J. Magnes. Alloys 13 (2025) 4817–4824.

[12] G.G. Wang, J.P. Weiler, J. Magnes. Alloys 11 (2023) 78–87.

[13] G.G. Wang, J. Bos, J. Magnes. Alloys 6 (2018) 114–120.

[14] J.P. Weiler, J. Magnes. Alloys 7 (2019) 297–304.

[15] E. Siemionek, K. Majerski, P. Surdacki et al., Adv. Sci. Technol. Res. J. 17 (2023) 245–253.

[16] J.P. Weiler, C. Sweet, A. Adams et al., Proc. IMA World Magnesium Conference, 2016.

[17] A.A. Luo, A.K. Sachdev, B.R. Powell, China Foundry 7 (2010) 463–469.

[18] N. Li, X. Chen, T. Hubbert et al., SAE Tech. Pap. 2005-01-0341, 2005.

[19] J. Song, J. She, D. Chen et al., J. Magnes. Alloys 8 (2020) 1–41.

[20] L. Zhan, Y. Sun, Y. Song et al., China Foundry 21 (2024) 525–545.

[21] G.G. Wang, J.P. Weiler, J. Magnes. Alloys 11 (2023) 78–87.

[22] G. Wang, J. Weiler, US Provisional Patent 63/316,608, 2022.

[23] J. Polmear, Mater. Sci. Technol. 10 (1994) 1–16.

[24] F.S. Pan, M.B. Yang, X.H. Chen, J. Mater. Sci. Technol. 32 (2016) 1211–1221.

[25] J. Kubásek, D. Dvorský, M. Čavojský et al., Kovove Mater. 57 (2019) 159–165.

[26] G. Chadha, J.E. Allison, J.W. Jones, Metall. Mater. Trans. A 38A (2007) 286–297.

[27] J.F. King, Magnesium Alloys and Their Applications, Wiley-VCH, 2006, pp. 14–22.

[28] A. Maltais, D. Dubé, M. Fiset et al., Mater. Charact. 52 (2004) 103–119.

[29] C. Blawert, N. Hort, K.U. Kainer, Trans. Indian Inst. Met. 57 (2004) 397–408.

[30] Jiang J. Design and analysis of Mg-Al alloy beam. Commercial Vehicle, 2022, 12: 84-85+100.

[31] I.J. Polmear, Mater. Sci. Technol. 10 (1994) 1–16.

[32] F.S. Pan, M.B. Yang, X.H. Chen, J. Mater. Sci. Technol. 32 (2016) 1211–1221.

[33] S.S. Park, Y.S. Park, N.J. Kim, Met. Mater. Int. 8 (2002) 551–554.

[34] L. Cížek, M. Greger, L. Pawlica et al., J. Mater. Process. Technol. 157–158 (2004) 466–471.

[35] D.S. Kumar, K.N.S. Suman, Int. J. Eng. Manuf. 4 (2014) 31–41.

[36] Y.L. Ma, Q.J. Chen, Y. Wang et al., Mater. Rep. 8 (2007) 84–87.

[37] Z. Tian, B. Song, Y.B. Liu, Autom. Technol. Mater. 7 (2004) 21–23.

[38] A.A. Luo, A.K. Sachdev, Adv. Wrought Magnesium Alloys, 2012, pp. 393–426.

[39] Li W, Kang S L, Wang H M. Based on the lightweight design of an electric vehicle console. Auto Sci-Tech., 2020, 3: 76-83.

[40] S. Zhang, J.F. Song, H.X. Liao et al., Materials 12 (2019) 1100.

[41] F. Mert, A. Özdemir, K.U. Kainer et al., Trans. Nonferrous Met. Soc. China 23 (2013) 66–72.

[42] B.R. Powell, A.A. Luo, P.E. Krajewski, Advanced Materials in Automotive Engineering, 2012, pp. 150–209.

[43] A.A. Luo, J. Renaud, I. Nakatsugawa et al., JOM 47 (1995) 28–31.

[44] F. He, J.P. Li, Z. Yang, Spec. Cast. Nonferrous Alloys 3 (2008) 227–229.

[45] S. Zhu, T.B. Abbott, J. Nie et al., J. Magnes. Alloys 9 (2021) 1537–1545.

[46] Y.F. Li, A. Zhang, C.M. Li et al., J. Mater. Res. Technol. 26 (2023) 2919–2940.

[47] Cui X P, Zhang Y X, Liu H F, et al. Development and application of magnesium alloy seat back for passenger cars. Foundry, 2022, 71(5): 637-644.

[48] F. Moll, M. Mekkaoui, S. Schumann et al., Proc. 6th Int. Conf. Magnesium Alloys, 2003, pp. 936–942.

[49] J.T. Carter, P.E. Krajewski, R. Verma, JOM 60 (2008) 77–81.

[50] Ren W, Li D P, Wang Z W, et al. Design of magnesium alloy seating riser. In: Proc. 2023 Chongqing Foundry Annual Conference, Chongqing, China, 2023: 367-370.

[51] N. Khademian, Y. Peimaei, 5th Int. Conf. Interdiscip. Stud. Nanotechnol., 2021, pp. 1–23.

[52] Q. Wang, Z.M. Zhang et al., Trans. Nonferrous Met. Soc. China 20 (2010) 599–603.

[53] Q. Wang, Z.M. Zhang et al., Trans. Nonferrous Met. Soc. China 18 (2008) 205–208.

[54] S.K. Kim, H.J. Yoo, Y.J. Kim, Magnesium Technology 2002, pp. 247–254.

[55] J. Liao, Adv. Mater. Res. 328 (2011) 213–219.

[56] J. Aragones, K. Goundan, S. Kolp et al., SAE Tech. Pap. 2005-01-0340, 2005.

[57] X. Chen, D. Wagner, G. Heath et al., SAE Technical Paper, 2021.